Adsorption of 2-mercaptobenzimidazole Corrosion Inhibitor on Copper: DFT Study on Model Oxidized Interfaces

Fatah Chiter, Dominique Costa, Vincent Maurice, Philippe Marcus

Journal of the Electrochemical Society

The Electrochemical Society
Advancing solid state & electrochemical science & technology

Adsorption of 2-mercaptobenzimidazole Corrosion Inhibitor on Copper: DFT Study on Model Oxidized Interfaces

Journal of The Electrochemical Society, 2020 **167** 161506

Adsorption of 2-mercaptobenzimidazole Corrosion Inhibitor on Copper: DFT Study on Model Oxidized Interfaces

Fatah Chiter,[z] Dominique Costa,[z] Vincent Maurice, and Philippe Marcus[*]

PSL Research University, CNRS—Chimie ParisTech, Institut de Recherche de Chimie Paris (IRCP), Physical Chemistry of Surfaces Group, 75005 Paris, France

High corrosion inhibition efficiency of the 2-mercaptobenzimidazole (MBI) molecule for copper in different aqueous solutions is well established. We propose a first principle DFT study of the surface chemistry of the adsorption of MBI on preoxidized Cu(111). For both thione (MBIH) and thiolate (MBI°) species, the formation of a full monolayer (ML) is favored over low coverage adsorption. At the ML coverage, the molecules adopt a perpendicular orientation with respect to the surface. MBI° interaction with the surface is stronger than MBIH one. MBIH and MBI° bond to the surface forming a S–Cu bond; for MBIH, the NH moiety forms a H-bond with a surface oxygen atom; for MBI°, a N–Cu bond is formed. For MBI° at low coverage, a Cu–C bond is also formed. The charge analyses show a charge transfer between the surface and the molecule. Comparing the MBIH/MBI° adsorption energies with that of water/OH, we find that MBI° can replace H_2O and OH at the preoxidized Cu surface. The results are compared with those obtained with 2-mercaptobenzothiazole, a similar azole derivative with corrosion inhibition properties.
 [DOI: 10.1149/1945-7111/abcd4f]

Manuscript submitted September 18, 2020; revised manuscript received November 19, 2020. Published December 7, 2020. *This paper is part of the JES Focus Issue on Characterization of Corrosion Processes in Honor of Philippe Marcus.*

Corrosion of copper has huge economic impact and affects many industrial domains. Its control by ⟪green⟫ inhibitors is the major concern in order to replace the standard corrosion inhibitors, that are often expensive, unstable, and in some cases highly toxic or dangerous for humans and/or the environment. It has been demonstrated that molecules that contain mercapto, benzene, and methyl groups are efficient corrosion inhibitors on copper.[1–6] Among these potential organic inhibitors, the 2-mercaptobenzimidazole (MBI) molecule is well known experimentally to have a good efficiency on copper surfaces but its adsorption mechanisms are still discussed. Quantum calculations are now often used to elucidate molecular properties and molecule-surface interactions to understand corrosion inhibition properties.[7–9]

High corrosion inhibition effectiveness of the MBI molecule was unequivocally demonstrated in different aqueous solutions. MBI exhibits very good inhibiting performance for copper corrosion in 3 wt.% aqueous NaCl solution,[2–4] in 0.5 M sulfuric acid[10] and in 1 M nitric acid solution,[6] where it acts as a mixed type (anodic and cathodic) inhibitor with a stronger effect on the anodic side.[3,4] MBI shows also promising anti-corrosion properties in neutral saline conditions on Cu, Fe and Pt anodes[11] and in alkaline methanol solution on Cu,[12] and it is established that the molecules form a continuous polymer (poly(MBI)) film on Cu. Izquierdo et al.[13] characterized the inhibiting effect of MBI on copper in chloride and sodium sulfate solutions, using scanning electrochemical microscopy (SECM). In the presence of chloride ions, MBI forms thicker and more insulating surface layers than in sodium sulfate solution. Zhang et al.[14] studied the corrosion behavior of copper in 0.5 M HCl containing three inhibitors, including MBI. They showed that MBI is the most effective one, and explained that, for example, benzotriazole (BTA) is less effective in acidic solutions due to the protonation of the molecule. Indeed, using various electrochemical techniques, it was shown that the inhibition effectiveness of MBI on copper is comparable in acid and alkaline solutions,[5] whereas BTA promotes inhibition only in neutral solution.[5,14]

Many experimental works have been devoted to the protective adsorption film formed by MBI on oxidized or metallic copper surfaces. It is established that MBI molecules self-assemble on the copper surface and form a protective barrier against corrosion in various experimental conditions. Using X-ray photoelectron spectroscopy (XPS) and Auger spectroscopy, Chadwick and Hashemi[1] studied the films formed by MBI or 2-mercaptobenzothiazole (MBT) molecules on copper. They evidenced the formation of a protective film under different experimental conditions and suggested a precipitation mechanism for Cu_2-MBI film formation. The film thickness of the protective layer is related to the stability and thickness of the Cu_2O oxide, wich depends on the pH regime. Xue et al.[15] determined, thanks to XPS and infrared spectroscopy (IR), that the reaction products forming an effective anti-corrosion film (Cu-MBI complex) on metallic copper under mild conditions are different from those forming a protective film on oxidized copper. The film can subsequently protect copper exposed in acid, alkaline and aggressive environments, as determined by cyclic voltammetry.[15] Several works suggested the formation of an organo-metallic polymer (Cu-MBI or Cu_2-MBI) film on copper[1,11,12,14,15] with both nitrogen and sulfur atoms involved in the reaction mechanism.

In order to investigate the surface chemistry of adsorbed MBI on copper, Finšgar[16] studied by XPS pure copper immersed in 3 wt.% NaCl solution containing 1 mM of MBI. The thickness of the organic layer formed on the Cu surface was found to be 1.9 ± 0.5 nm. MBI bonded to the oxidized Cu surface through N and S atoms and the author suggested a bidentate binding –N–S–bridge connection as the most likely bonding configuration. Milošev et al.[3] suggested that the sulfur and the pyridine N atoms point toward the metal surfaces. However, Niamien et al.[17] proposed that the adsorption of some benzimidazole derivatives, including MBI, on copper involves both physisorption and chemisorption interactions.

Despite the strong interaction of MBI on copper surfaces in different aqueous conditions and the formation of a protective film being well established, the nature of the adsorption of the molecule is not clearly defined and some points remain still to be clarified. Following a standard QSAR (Quantitative Structure Activity Relationship) approach, the corrosion inhibition properties of MBI were investigated relative to the electronic properties of the isolated molecule.[6,8,14,17] However, the correlation between experimental and electronic properties of isolated molecules can only be considered as a first indicator of the reactivity of the molecules since the approach is not sufficient to describe precisely the inhibition efficiency on a given substrate surface, which is more complex,

*Electrochemical Society Fellow.
[z]E-mail: fatah.chiter@chimieparistech.psl.eu; dominique.costa@chimieparistech.psl.eu

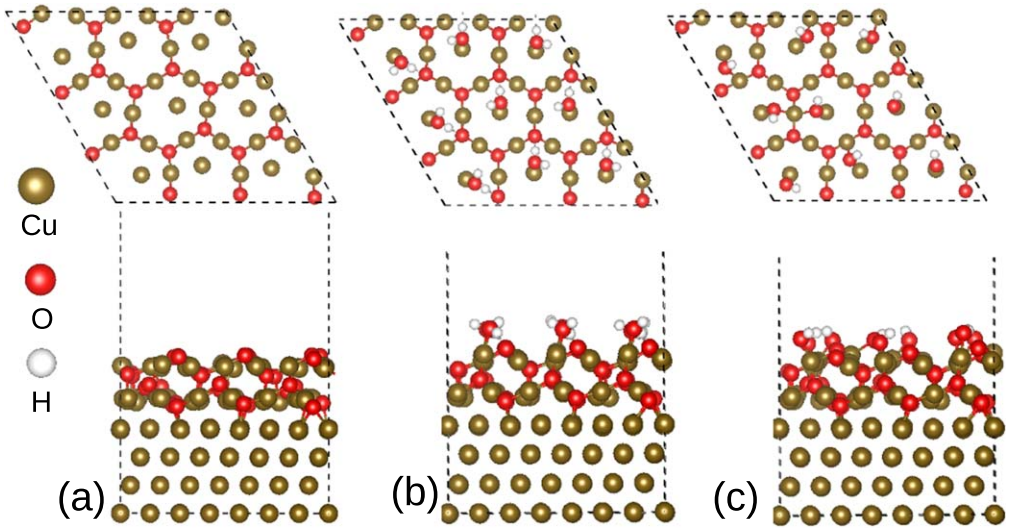

Figure 1. Snapshots of the preoxidized copper surface (Cu(111)|| Cu_2O(111)) with different oxide surface states (top view and side view). (a) dry, (b) hydrated and (c) hydroxylated surface states.

especially to describe the interfacial chemistry of the adsorbed system. Therefore, some Density Functional Theory (DFT) studies addressed the direct interaction of MBI on metallic copper surfaces. Sun et al.[9] modeled by DFT the adsorption of three potential inhibitors including MBI onto the clean Cu(111) surface at low coverage and concluded to a chemisorption strength order consistent with the experimental results of inhibiting efficiency. The thiol form of MBI was found physisorbed in parallel configuration and weakly chemisorbed in perpendicular configuration, whereas the dehydrogenated form (thiolate) was found strongly chemisorbed on the surface with both perpendicular and tilted adsorption configurations through N–Cu and/or S–Cu bond. Obot et al.[18] studied by DFT and molecular dynamics (MD) simulations the adsorption of MBI on Fe (110), Al(111) and Cu(111) surfaces at low coverage. They concluded that the thiol species is less stable than the thione species and the molecule binds spontaneously to the surface in a parallel configuration via the S and N reaction sites and the π electrons of the molecule. Kovačević et al.[7] also used DFT calculations to study the corrosion inhibition properties of five imidazole molecules, including MBI, on copper surfaces and hydrated Cu^{2+} ions. They confirmed that thione tautomers of mercapto molecules are more stable in gaseous as well as aqueous phases and also bond stronger to the copper surface than thiol forms. However, the thiol form was found to be very prone to dissociation upon adsorption and the dissociated (deprotonated) thiolate species to bind to the Cu atoms via S and N atoms. The calculations also revealed that standalone adsorbed molecules are thermodynamically more stable than organometallic adcomplexes. In contrast to other molecules, MBI molecules do not react with Cu^{2+} ions to form soluble complexes which would promote corrosion. Vernack et al.[19] studied adsorption of MBI in thiol, thione and thiolate forms on Cu(111). They found that the adsorption of the thiolate form is favored, with the formation of S–Cu and N–Cu bonds, independently of the surface coverage. Several tentative superstructures were compared and the most favored was the (3×3) superstructure with a molecule density of 3.9 molecule nm^{-2}.

All these theoretical results are important to understand the reactivity of MBI and to describe inhibitor-surface bonding on bare metallic surfaces. However, these model studies are inappropriate to describe the inhibition properties of MBI observed in neutral and alkaline conditions where copper is covered by an ultrathin passive oxide film. In particular, it has been shown that the protective film formed by MBI depends on the stability and thickness of the Cu_2O oxide.[1,15,16] Here we performed quantum chemical DFT calculations of the interaction mechanism of MBI in thione or thiolate forms on Cu(111) surface covered by an ultrathin Cu_2O oxide film (Cu(111)|| Cu_2O(111)) derived from experimental data. The MBI species were adsorbed at low and full coverage and the adsorption configurations and energies were systematically investigated. In addition we confirmed the adsorption mode of each species by electronic properties analysis. MBI adsorption is compared to water/OH adsorption in order to study in which conditions MBI is adsorbed at the solid/liquid interface with the passivated surface. Comparative analysis with our results obtained with MBT,[20] also an azole derivative known as efficient inhibitor for copper corrosion, on the same model of oxidized copper, is given.

Computational Details

All calculations were performed in the framework of DFT with the periodic plane-wave basis set code VASP (Vienna Ab initio Simulation Package).[21–24] The calculations conditions were similar as in Ref. 20 and we refer to this publication for computational details. Here we recall that the calculations were performed

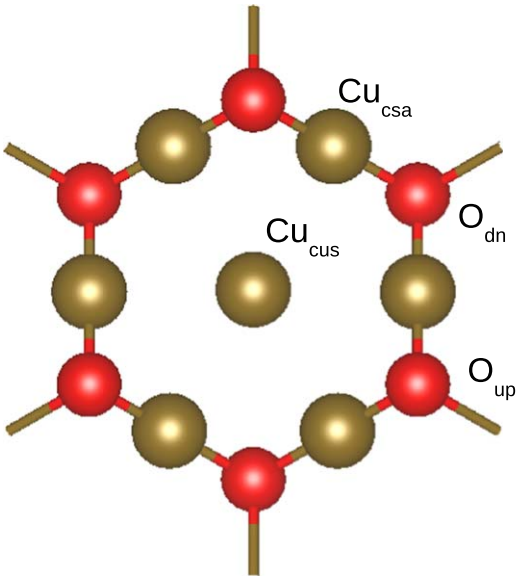

Figure 2. Sites on Cu_2O(111) surface. Unsaturated (Cu_{cus}) and saturated (Cu_{csa}) copper surface sites and unsaturated (O_{up}) and saturated (O_{dn}) oxygen surface sites.

including dispersion forces at the OptB86b-vdw level,[25] offering a good compromise for the lattice parameters of bulk Cu-metal and Cu_2O-oxide with equilibrium values of 3.599 (−0.30%) and 4.272 Å (+0.05%), in good agreement with experimental values of 3.61[26] and 4.27 Å,[27] respectively.

Model.—The construction and properties of the Cu(111)|| Cu_2O(111) model were studied previously,[28] and we refer to this work for more description details. The metal is represented by four Cu(111) planes and the oxide film by two stoichiometric Cu_2O(111) layers (thickness of 5.89 Å) and corresponds to a (7 × 7) supercell for Cu(111) matching to a (6 × 6) supercell for Cu_2O(111).

The large cell size allowed us to model several surface coverages, 0.37 (low surface coverage) and 3.27 (high surface coverage) molecule nm^{-2}. In order to study the substitution mechanism of adsorbed water molecules and condensation mechanism on surface OH groups, three surface states of the oxide layer were considered for the adsorption of the MBI molecule, as shown in Figs. 1a, 1b and 1c for the dry, hydrated and hydroxylated surface states, respectively, and the different sites of dry surface state are illustrated in Fig. 2.

MBI molecule.—The MBI molecule was modeled in thione (MBIH) and radical thiolate (MBI°) forms (Fig. 3). The carbon atoms 1–6 correspond to the benzene ring with C_1 and C_2 being attached to the nitrogen N_1 and N_2, respectively. C_7 is the carbon atom in the hetero-cyclic ring attached to the two nitrogen and the sulfur atoms. The MBI molecules were adsorbed on top of the oxide layer. The isolated molecules were optimised in a box (1 molecule/box) with dimensions of 20 Å × 20 Å × 20 Å, using the computational conditions described above, except for the radical MBI° form, where unrestricted spin was implemented to get the energy minimum.

The energetic, structural and tautomeric properties of the MBI molecule have been described in the literature. The cohesion of the molecules in the crystals is due to intermolecular N–H...S H-bonding network.[29] The thione form would be the preferred form in gaseous phase.[30] The thione tautomer shows higher reactivity than the thiol tautomer in both vacuum and aqueous phases and the ionized thiolate form exhibits the strongest reactivity.[31] So, the thiol species was not considered here. The ability of MBI to donate electrons (HOMO position relative to the Fermi level), to accept electrons (LUMO position relative to the Fermi level) and to react (gap between HOMO and LUMO) with metal surfaces was studied using quantum chemical calculations[17,32] as well as the electronegativity (χ) and global hardness (γ).

Energetics.—The adsorption energy of the thione form (MBIH) was calculated as:

$$E_{ads} = [E(\text{slab/MBIH}) - E(\text{slab}) - nE(\text{MBIH})]/n \quad [1]$$

where E(slab/MBIH) is the total energy of the system with MBIH adsorbed on the slab surface. E(slab) and E(MBIH) are the energies of the bare, relaxed Cu(111)|| Cu_2O(111) slab and of the free MBIH molecule optimized in vacuum, respectively. n is the number of molecules on the surface.

The adsorption energy for the radical thiolate form (MBI°) was calculated as:

$$E_{ads} = [E(\text{slab/MBI°}) - E(\text{slab}) - nE(\text{MBI°})]/n \quad [2]$$

where E(slab/MBI°) is the total energy of the system with MBI° adsorbed on the slab surface. E(MBI°) is the energy of the free radical MBI° optimized in vacuum and n is the number of radical adsorbates on the surface.

In order to compare the stability of a dense layer adsorbed at full coverage with the adsorption at low coverage, we normalized the adsorption energy per unit area as follows:

$$\varepsilon_{norm} = E_{ads} \times \theta \quad [3]$$

where E_{ads} is the adsorption energy per molecule and $\theta = \frac{n}{A}$ is the coverage, defined as the number of adsorbed molecules (n) per area (A) of the slab.

We evaluated the interaction of MBIH and MBI° with the hydrated surface considering a substitution reaction, where MBI replaces H_2O on the surface covered initially by water molecules and water molecules are released after adsorption. The reaction is:

$$\text{MBI} + \text{H}_2\text{O}_{ads} \longrightarrow \text{MBI}_{ads} + \text{H}_2\text{O} \quad [4]$$

where H_2O_{ads} stands for adsorbed H_2O molecules and MBI_{ads} for adsorbed MBI molecules (MBIH or MBI° form). The corresponding substitution energy is calculated as:

$$\Delta E_{subst} = [E(\text{slab/MBI}) + nE(\text{H}_2\text{O}) - E(\text{slab/H}_2\text{O}) - nE(\text{MBI})]/n \quad [5]$$

where E(slab/MBI) is the total energy of the system with MBI (MBIH or MBI°) adsorbed on the slab surface. $E(H_2O)$ is the energy of a water molecule calculated in the vacuum. E(slab/H_2O) and E(MBI) are the energies of the optimized structures with the water molecules adsorbed on the surface and the free MBIH or MBI° form optimized in vacuum, respectively. n is the number of adsorbed (or released) molecules.

We also evaluated the interaction of the thione form (MBIH) with the hydroxylated surface. The following condensation reaction (replacement of an OH group by the MBI° form and release of water molecule) was considered:

$$\text{MBIH} + \text{OH}_{ads} \longrightarrow \text{MBI}_{ads} + \text{H}_2\text{O} \quad [6]$$

where OH_{ads} stands for a surface OH group and MBI_{ads} for an adsorbed molecule under thiolate form after reaction. The corresponding condensation energy is calculated as:

$$\Delta E_{cond.} = [E(\text{slab/MBI°}) + nE(\text{H}_2\text{O}) - E(\text{slab/OH}) - nE(\text{MBIH})]/n \quad [7]$$

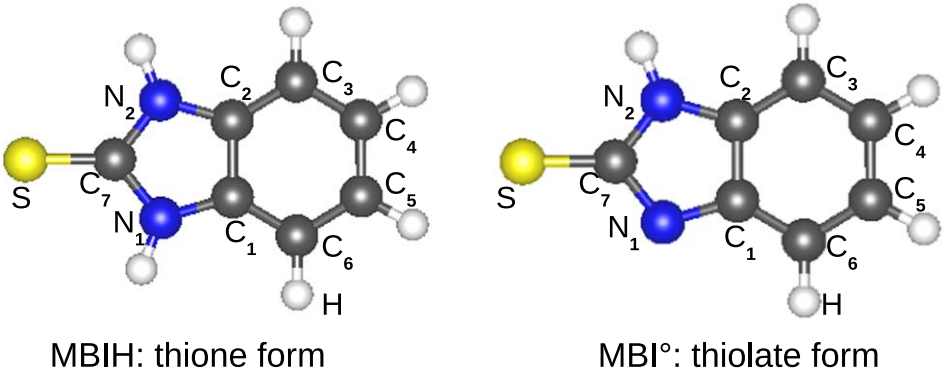

Figure 3. Thione (MBIH) and thiolate (MBI°) species of MBI molecule at isolated state. Carbon atoms 1–6 correspond to the benzene ring with C_1 and C_2 being attached to the nitrogen N_1 and N_2, respectively. C_7 is the carbon atom in the hetero-cyclic ring attached to the two nitrogen and the sulfur atoms.

Table I. Adsorption of MBI on preoxidized copper surface (Cu (111)|| Cu_2O(111)) at low coverage. E_{ads} is the adsorption energy on the dry surface, using Eqs. 1 and 2 for MBIH and MBI°, respectively. ε_{norm} is the adsorption energy normalized per unit area, using Eq. 3.

Low coverage (0.37 molecule nm^{-2})	E_{ads} (eV $molecule^{-1}$)	ε_{norm} (J m^{-2})	Figures
MBIH	−2.84	−0.16	Fig. 4a
	−2.66	−0.15	Fig. 4b
MBI°	−4.14	−0.24	Fig. 5a
	−2.06	−0.12	Fig. 5b

where E(slab/MBI°) is the total energy of the system with MBI thiolate (MBI°) adsorbed on the oxide surface. E(slab/OH) is the energy of the optimized hydroxylated slab surface. n is the number of adsorbed MBI molecules.

Electronic and charge analysis.—We plotted the charge density difference expressed as follows:

$$\Delta\rho(r) = \rho(r)_{slab/mol} - (\rho(r)_{slab} + \rho(r)_{mol}) \quad [8]$$

where $\rho(r)_{slab/mol}$ is the charge density distribution on the adsorbed system. $\rho(r)_{slab}$ and $\rho(r)_{mol}$ are the charge density distributions on the isolated slab and the molecule for the geometry after adsorption, respectively.

The net charge variation was determined on each atom by:

$$\Delta Q(x) = Q_{ads}(x) - Q_{vac}(x) \quad [9]$$

where $Q_{ads}(x)$ and $Q_{vac}(x)$ are the net charges on each atom (Bader population analysis)[33] of the adsorbed and free molecule, respectively.

Results and Discussion

Adsorption modes and energetics.—We aimed at determining if the molecules interact on the preoxidized copper surface and what are the most favored adsorption modes for MBIH and MBI° species at full monolayer. We considered three surface states: dry, hydrated and hydroxylated. Like in our previous work on MBT molecule adsorbed on the same system[20] we tested the most relevant adsorption configurations.

Adsorption of thione (MBIH) and thiolate (MBI°) forms at low coverage (0.37 molecule nm^{-2}).—Table I compiles the adsorption energy values calculated at low coverage (0.37 molecule nm^{-2}) for the MBIH and MBI° forms. Figures 4 and 5 show the corresponding adsorption configurations of the thione and thiolate forms at low coverage, respectively.

The most stable configuration obtained at low coverage for MBIH is showed in Fig. 4a. We calculated an adsorption energy of −2.84 eV $molecule^{-1}$ and ε_{norm} of −0.16 J m^{-2}. MBIH binds covalently via the S atom to a Cu_{cus} atom with a bond length of 2.16 Å. One NH group of the MBIH forms a H-bond with an O_{up} atom, whith a distance NH...O of 1.57 Å. The molecule plane is tilted toward the surface as compared to the perpendicular adsorption in Fig. 4b. In the perpendicular adsorption, MBIH adsorbs via similar sites but the adsorption is less stable by 0.18 eV $molecule^{-1}$. The energy difference originates from the contribution of the Van der Waals interactions between the molecule and the surface.

The reactivity for the thiolate form is different since the molecule can form a H-bond with a surface oxygen via the NH group and can also interact directly with surface copper atoms via the nitrogen atom from the deprotonated NH group, in addition to the bonding via the sulfur atom. For MBI° at low coverage, the most stable adsorption configuration is shown in Fig. 5a. MBI° is in a tilted orientation toward the surface with the molecule plane highly tilted to the surface, like for the most stable configuration of MBIH (Fig. 4a), However the MBI° adsorption involves different adsorption sites. Indeed, MBI° binds via the S atom to Cu_{cus} atom with a bond length of 2.16 Å, and one carbon atom in the aromatic ring (C_3 in Fig. 3b) is also involved in the interaction mechanism with a bond lengths C...Cu_{cus} of 2.11 Å. MBI° also forms a covalent bond via the nitrogen atom with a saturated copper atom with a bond length of 2.08 Å. The adsorption energy is −4.14 eV $molecule^{-1}$ ($\varepsilon_{norm} = -0.24$ J m^{-2}). This is more stable by 2.08 eV $molecule^{-1}$ than for the MBI° adsorption configuration in Fig. 5b, with a NH...O_{up} H-bond instead of a N...Cu_{csa} covalent bond.

Comparison between the two forms of MBI adsorbed at low coverage indicates different adsorption sites and more stable adsorption for MBI° in the presence of both species (thione and thiolate) in the reacting phase ($\Delta E_{ads} = 1.30$ eV $molecule^{-1}$). In order to better understand the competitive adsorption of both forms, we considered the following mechanisms, where MBIH dissociates at the surface, releasing one H atom. The H atom can either be released as gaseous dihydrogen, or be co-adsorbed with MBI at the surface ($MBIH + * \longrightarrow MBI_{ads} + \frac{1}{2} H_2$ or $MBIH + * \longrightarrow MBI_{ads} + H_{ads}$). We calculated adsorption energies of −2.61 and −3.55 eV $molecule^{-1}$ for the first and the second mechanisms, respectively, which indicates that the dissociation of MBIH species on the Cu(111)|| Cu_2O(111) dry surface is exothermic for the two mechanisms. The second mechanism even shows that the dissociative adsorption of the molecule (−3.55 eV $molecule^{-1}$) is more stable than the intact adsorption (−2.84 eV $molecule^{-1}$). We can conclude that the adsorption of MBI on the oxidized copper surface is favored in the thiolate form (MBI°). This contrasts with the results obtained with MBT that showed that the dissociative adsorption of MBTH on oxidized copper surface is not favored and the competitive adsorption of MBT° is favored only in the presence of both species (thione and thiolate) in the reacting phase.[20] In terms of adsorption energy, MBT adsorption is favored over MBI adsorption at low coverage for both thione and thiolate forms.

Comparison of our results with those for the interaction of MBI with the metallic copper surface at low coverage reveals that the adsorption of MBI on the oxidized copper surface is more stable than on the metallic copper surface. Kovačević et al.[7] calculated a binding energy of −2.49 eV for thiolate form and an adsorption energy of −0.77 and −0.48 eV $molecule^{-1}$ for thione and thiol MBI forms, respectively, on metallic copper. They also showed that the dissociation of the molecules is thermodynamically favorable and kinetically feasible, with an activation barriers of 0.15 and 0.9 eV for thiol (S–H bond) and thione (N–H bond) forms, respectively,[7] which reveals that the S–H bond cleavage of thiol is way easier than the N–H bond cleavage of thione. The adsorption energy of the molecule under thiolate form is −2.40 eV $molecule^{-1}$[19] and the interaction with metallic copper involves both S and N atoms. Vernack et al.[19] calculated an adsorption energy of −1.25 eV $molecule^{-1}$ for the thiolate form on Cu(111) at low coverage, also less favorable than that calculated in the present work for the adsorption on the oxidized copper surface.

Adsorption of thione (MBIH) and thiolate (MBI°) forms at high coverage (3.27 molecule nm^{-2}).—Table II compiles the different energy values calculated (3.27 molecule nm^{-2}) for the MBIH and MBI° forms adsorbed at high coverage on Cu(111) covered by two Cu_2O(111) oxide layers. Figures 6 and 7 show the corresponding adsorption configurations of the thione and thiolate forms, respectively.

For MBIH at full coverage, the S atom and the NH group are directed toward the surface in the most stable configuration and the molecules stand with their plane perpendicular to the surface (Fig. 6a). The adsorption energy is −2.76 eV $molecule^{-1}$ and is less favorable than at low coverage. However, the normalization of the adsorption energy to a unit area, $\varepsilon_{norm} = -1.45$ J m^{-2}, shows that the formation of a full monolayer is markedly favored compared to the adsorption at low coverage. MBIH forms a covalent bond via

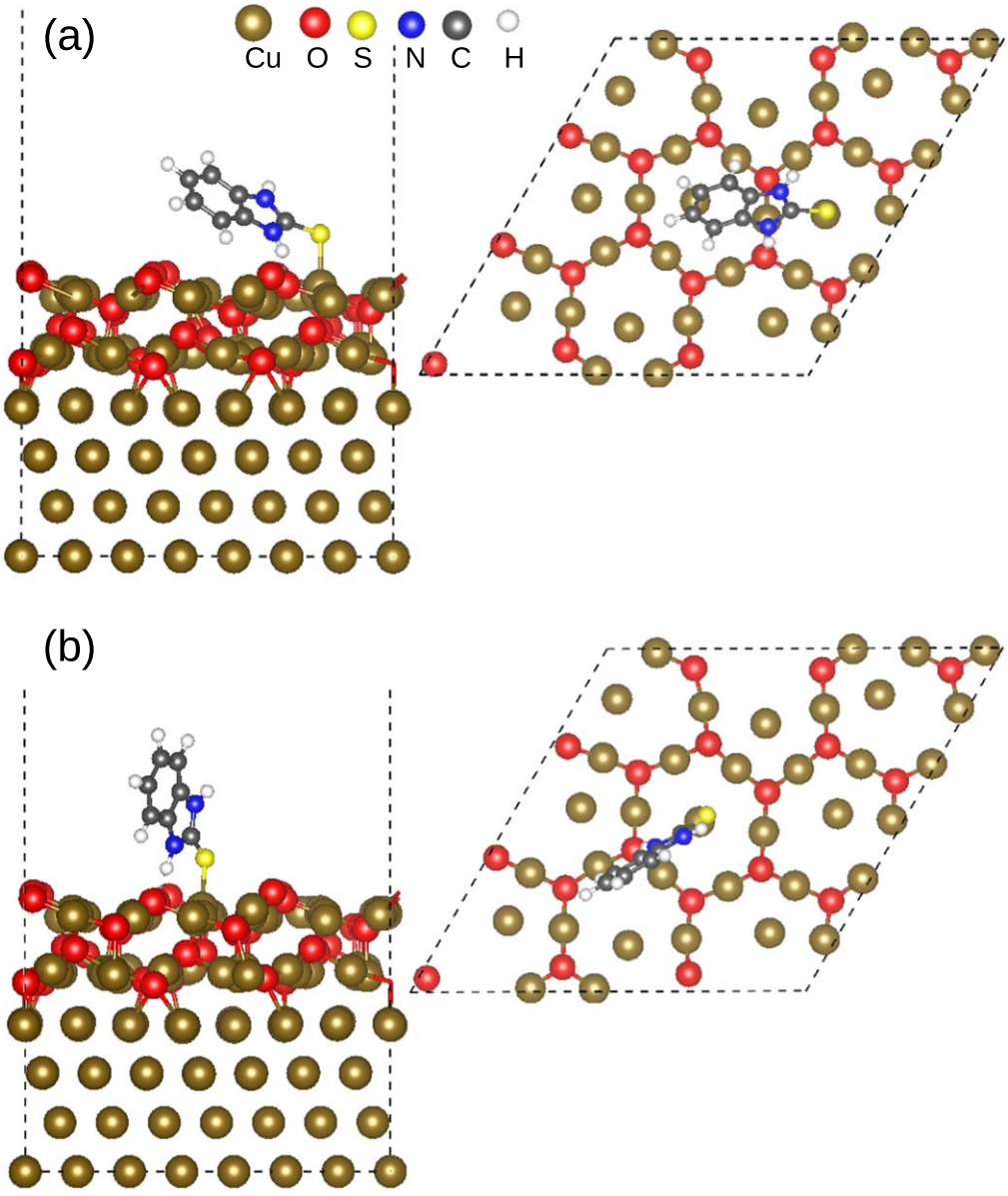

Figure 4. Snapshots of two adsorbed configurations of thione form (MBIH) at low coverage (0.37 molecule nm^{-2}). (a) tilted adsorption and (b) perpendicular adsorption on preoxidized copper surface (Cu(111)|| Cu_2O(111)).

the S atom to a Cu_{cus} atom with a S–Cu_{cus} bond length of 2.15 Å and a H-bond between the NH group and an unsaturated oxygen (O_{up}) atom with a distance NH...O of 1.50 ± 0.05 Å. The adsorption direction from Cu_{cus} to O_{up} (Fig. 6a) is favored over Cu_{cus} to O_{dn} (Fig. 6b) by the formation of the H-bond.

For MBI° at full coverage, the molecule adsorbs also in a perpendicular orientation like the MBIH form. However, the thiolate form can be adsorbed via S and N atoms or via S atom and NH group, the two configurations being noted (a) and (b) in Fig. 7, respectively. In the most stable configuration (Fig. 7a), the S and the N atoms of the molecules are directed toward the surface. MBI° forms two covalent bonds, via the S atom to an unsaturated copper atom, with a bond length of 2.12 Å, and via the N atom to a saturated copper atom, with a bond length of 2.05 ± 0.07 Å. The adsorption energy is −3.34 eV $molecule^{-1}$. Again, the normalization to unit area of the adsorption energy shows that the full monolayer adsorption ($\varepsilon_{norm} = -1.75\ J\ m^{-2}$) is favored compared to the adsorption at low coverage ($\varepsilon_{norm} = -0.24\ J\ m^{-2}$). For the less stable configuration (Fig. 7b), the adsorption energy is −2.99 eV $molecule^{-1}$ ($\varepsilon_{norm} - 1.57 = J\ m^{-2}$). The S atom and NH groups are directed toward the surface and the molecule is oriented from Cu_{cus} to O_{up} direction on the surface, which favors the formation of a H-bond between the NH group and a O_{up} atom, with a distance NH...O_{up} of 1.67 ± 0.05 Å. In addition, MBI° binds via its S atom to an unsaturated copper atom, with a bond length of 2.14 Å.

Comparison for full coverage between MBIH and MBI° species indicates different reaction sites. For the MBIH form, only the sulfur atom is involved in the formation of a covalent bond, while for the MBI° form, both sulfur and nitrogen atoms are involved in the formation of chemical bonds with the surface. We found lower adsorption energy for MBI° than for MBIH ($\Delta E = 0.58$ eV $molecule^{-1}$), like for MBT° compared to MBTH on the same surface.[20] This competitive adsorption is valid in the presence of both forms of the molecule in the same medium, as discussed for the low coverage case. However, the adsorption energy of thiolate form (Table II) calculated under the mechanism MBIH + * ⟶ $MBI_{ads} + \frac{1}{2} H_2$ shows that the deprotonation of the molecule and desorption of dihydrogen is less stable than the adsorption of the intact MBIH molecule. Note that the surface reconstruction induced by the MBI molecule under thione and thiolate forms is similar to

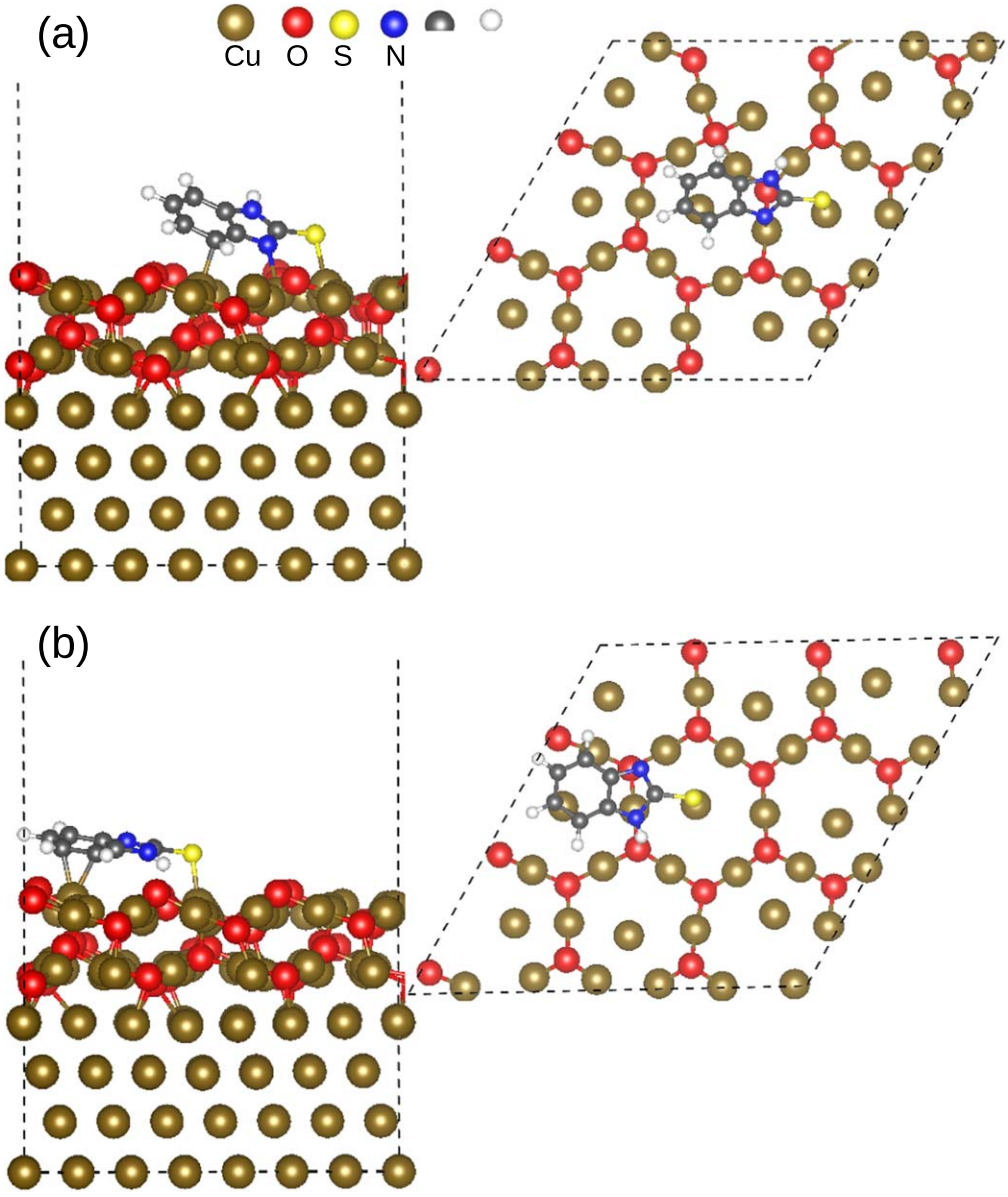

Figure 5. Snapshots of two adsorbed configurations of thiolate form (MBI°) at low coverage (0.37 molecule nm^{-2}). (a) adsorption via S, C and N atoms and (b) adsorption via S and C atoms and NH group on preoxidized copper surface (Cu(111)|| Cu_2O(111)).

Table II. Adsorption of MBI on preoxidized copper surface (Cu(111)|| Cu_2O(111)) at full coverage. E_{ads} is the adsorption energy on the dry surface using Eqs. 1 and 2 for MBIH and MBI°, respectively. ε_{norm} is the adsorption energy normalized per unit area (Eq. 3). $\Delta E_{sub.}$ and $\Delta E_{cond.}$ are the energies of substitution on the hydrated surface (Eq. 5) and condensation on the hydroxylated surface (Eq. 7), respectively. The values in brackets correspond to the adsorption energy of thiolate form under the following mechanism: MBIH + * $\longrightarrow$ MBI_{ads} + $\frac{1}{2}$ H_2.

High coverage (3.27 molecule nm^{-2})	E_{ads} (eV $molecule^{-1}$)	ε_{norm} (J m^{-2})	ΔE_{sub} (eV $molecule^{-1}$)	ΔE_{cond} (eV $molecule^{-1}$)	Figures
MBIH	−2.76	−1.45	−1.66	—	Fig. 6a
	−2.42	−1.27	−1.31	—	Fig. 6b
MBI°	−3.34 (−1.63)	−1.75 (−0.86)	−2.24	−1.56	Fig. 7a
	−2.99 (−1.29)	−1.57 (−0.67)	−1.89	−1.21	Fig. 7b

that found for the MBT molecule. The details given in Ref. 20 are not repeated here.

Adsorption of MBI molecule on hydrated and hydroxylated surfaces at high coverage (3.27 molecule nm^{-2}).—On the hydrated copper oxide surface, the substitution of the water molecule by MBIH or MBI° forms according to the mechanism defined in Eq. 4 and calculated with Eq. 5 was found exothermic. We calculated substitution energies of −1.66 and −2.24 eV $molecule^{-1}$ for the most stable monolayer configuration of MBIH (Fig. 6a) and MBI° (Fig. 7a), respectively, (Table II). This means that both forms of the MBI molecule are able to substitute the water molecules on the

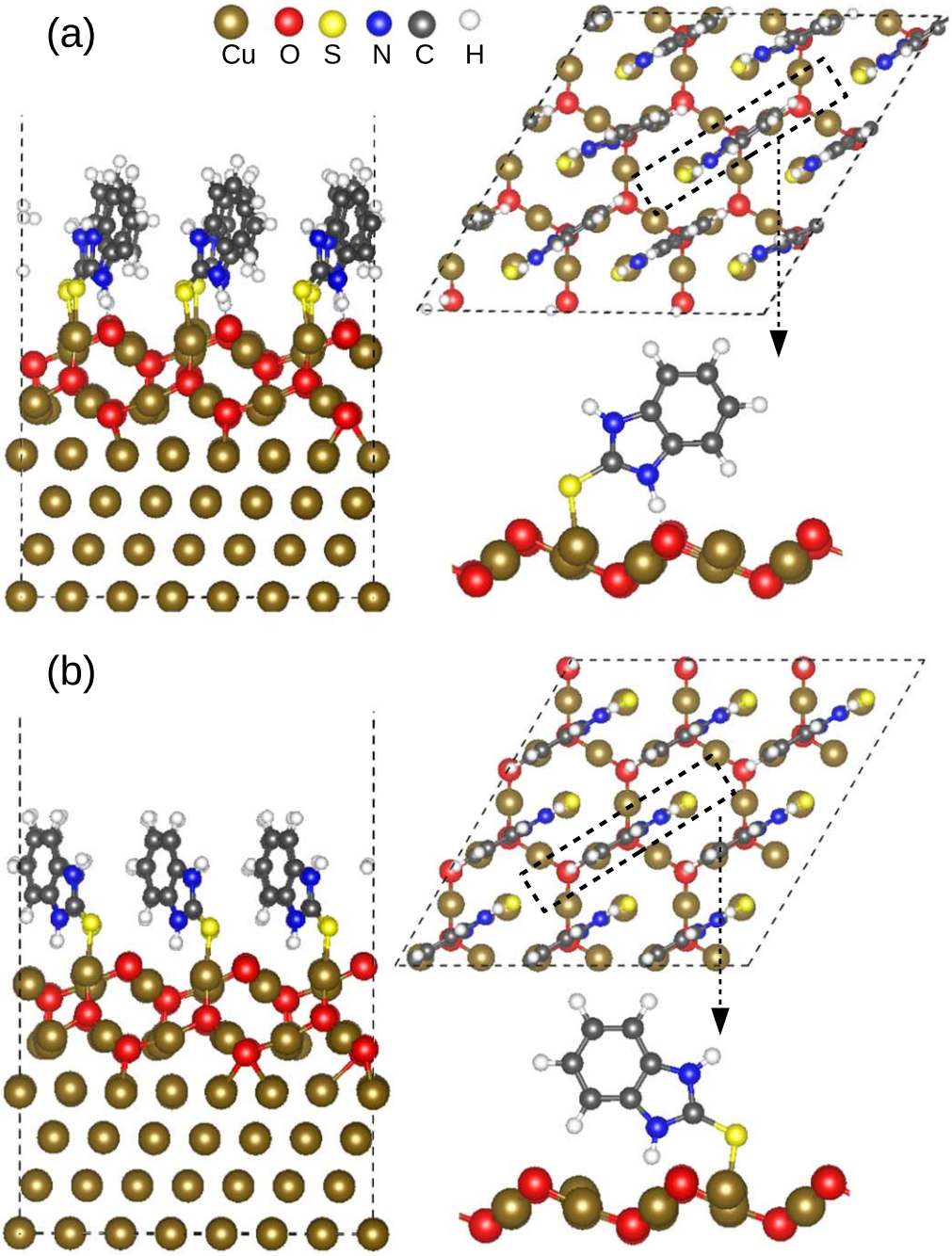

Figure 6. Snapshots of two adsorbed configurations of thione form (MBIH) at full coverage (3.27 molecule nm^{-2}). (a) adsorption via S atom and NH group and (b) adsorption via S atom on preoxidized copper surface (Cu(111)|| Cu_2O(111)).

hydrated copper oxide surface and to form a stable organic monolayer on the oxidized copper surface.

On the hydroxylated copper oxide surface, the substitution mechanism of hydroxyl groups, $OH_{ads} + MBI \longrightarrow MBI_{ads} + OH$, was found unfavored for both the MBIH and MBI° forms. Indeed, we calculated adsorption energies of 0.96 and 0.37 eV $molecule^{-1}$ for MBIH and MBI°, respectively, which indicate an endothermic process. However, the condensation reaction defined in Eq. 6 with the corresponding energy calculated by Eq. 7 showed that this mechanism is suitable. The condensation reaction is very exothermic with a calculated energy of −1.56 eV $molecule^{-1}$ for the most stable configuration (Fig. 7a). These simulations suggest that the MBIH form would be able to replace surface OH groups by forming adsorbed MBI° and releasing a H_2O molecule, but that the MBI° form would not be able to directly substitute surface OH group. These results reveal that the organic monolayer adsorbed on the hydroxylated surface of oxidized copper would consist of MBI° species and display strong adsorption bonding.

These calculations also reveal that the MBI molecule favors the formation of a stable, dense and ordered organic barrier on the oxidized Cu(111) surface under different surface states, with a density of 3.27 molecule nm^{-2}, rather than low coverage adsorption. This is in agreement with the experimental results, from which the formation of the protective film on copper under different experimental conditions was concluded as detailed in the Introduction section. However, we find that the composition of the organic layer and the orientation and the adsorption of the molecule on the surface depend on both the nature of MBI species present and the surface state of the copper in the medium. Musiani and Mengoli[5] studied the influence of pH and electrode potential on the effectiveness of some

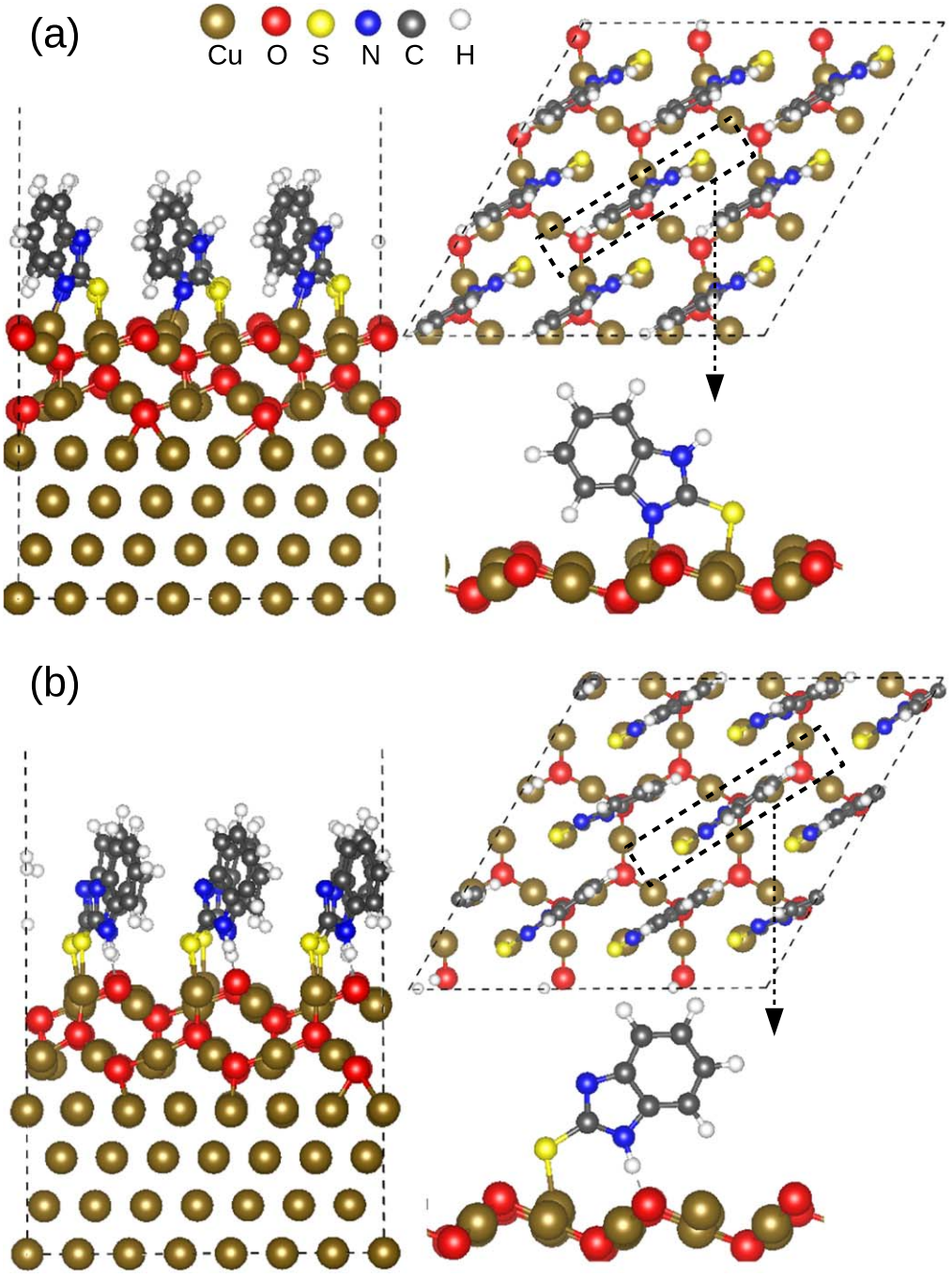

Figure 7. Snapshots of two adsorbed configurations of thiolate form (MBI°) at full coverage (3.27 molecule nm^{-2}). (a) adsorption via S and N atoms and (b) adsorption via S and NH group on preoxidized copper surface (Cu(111)|| Cu_2O(111)).

corrosion inhibitors, including MBI on copper, and concluded that the undissociated molecules and their anions are adsorbed simultaneously on the surface. MBI has a pK_a of 10 meaning that it is present as deprotonated form (thiolate) in solution of pH > 10. The molecule interacts via both S and N atoms to unsaturated and saturated copper atoms, respectively, on dry and hydrated Cu(111)|| Cu_2O surfaces but MBI° is unable to substitute directly OH groups on hydroxylated surfaces. At pH < 10, MBI is present in solution in the protonated form with predominance of thione (MBIH) species. MBIH binds only via S atom to unsaturated copper atom and the orientation of the molecule favors the formation of H-bond between the NH group and oxygen atom of the surface. However on hydroxylated Cu(111)|| Cu_2O surfaces, the MBIH molecule could be deprotonated and adsorbed on the surface more favorably in the thiolate form. In fact, our results demonstrate that the film formed by thiolate form is more stable than the film formed by thione species on oxidized copper surface, which could explain the results reported experimentally that both S and N atoms are involved in the interaction mechanism of MBI on oxidized copper surfaces.[3,16]

Experimentally, the corrosion inhibition effectiveness of MBI was also compared to other corrosion inhibitors like MBT.[1,10] The investigation of the surface chemistry of the adsorbed MBT corrosion inhibitor on oxidized copper surface was done in our previous work.[20] Comparison between the two molecules shows similar orientation and adsorption sites of the molecules in the film formed on the oxidized copper surface. The adsorption energies are identical for the thione form and more stable (by 0.20 eV) for MBI thiolate form than MBT thiolate form.

Electronic structure analysis.—In order to bring more insight into the molecule-surface interaction, we analyzed the electronic structure, which provides relevant information about the reactive sites of the molecules and the electronic exchange with the substrate surface. We plotted the density of states (DOS) and the projected density of states (PDOS), for the isolated molecules and adsorbed systems. We also analyzed the charge density variation ($\Delta\rho(r)$) defined in Eq. 8 to confirm the nature of the bonding.

Isolated species (before adsorption).—The total density of state (DOS) analysis of the isolated thione (MBIH) form is shown in Fig. 8a. For the radical thiolate (MBI°) form with an odd number of electrons, spin polarized (up and down) DOS is shown in Fig. 9a. Since the molecules contain S, N, C and H atoms, we projected the density of states (PDOS) for each type of atom susceptible to interact with the substrate surface. The results for the S and N atoms are shown in Figs. 8b and 9b for MBIH and MBI°, respectively. We take E_F, the Fermi level of the slab, as reference for the DOS and PDOS of the isolated molecules. To do so a single point calculation was performed with the free molecules in their optimized geometries and set parallel to the surface substrate at a vertical distance of 10 Å. This distance was large enough to prevent interaction between the molecule and the substrate, and this allows a clear identification of different orbitals contribution (HOMO and LUMO) of the isolated molecules in the occupied and unoccupied states of the DOS and PDOS.

For the isolated MBIH in Fig. 8a, the peaks located at about −0.05 and −0.20 eV below the Fermi level corresponds to the HOMO and HOMO-1 and the peak located at 3.12 eV above the Fermi level corresponds to the LUMO. The alignment of the HOMO and LUMO relative to Fermi level of the slab suggests that MBIH can behave more as an electron donor than as an acceptor during the adsorption process, which confirms the electron transfer from the molecule to the substrate discussed below. In contrast, the DOS analyses for the isolated MBI° in Fig. 9a suggests that the radical MBI° can behave as an electron donor or electron acceptor during the adsorption process. Indeed, the DOS shows that the semi full and semi empty orbitals are located near the Fermi level at about −0.55 and 0.05 eV, respectively. Because the radical MBI° lacks an electron as isolated species, the adsorption process favors an electron transfer from the substrate to the molecule as discussed below for MBI°.

For both MBI species, the PDOSs reveal that the occupied states near the Fermi level are dominated by the contribution of the sulfur orbitals (green line in Figs. 8b and 9b). Thus, the sulfur atom is the most reactive site in the MBI molecule and it is the most likely to chemically bond with the copper surface atoms. For MBIH (Fig. 8b), we observed a small contribution of the nitrogen atoms of the NH groups to the DOS, which is visible in the energies range [−1.40 −1.25] and [−0.25 0.00]. The PDOS shows a similar contribution for the two nitrogen atoms, due to the same chemical environment of the two NH groups in the molecule. In contrast for MBI°, we observed a higher contribution of the nitrogen orbitals for the dehydrogenated NH group than for the NH group, due to the different chemical environments of the two N atoms. It is visible at the semi full and semi empty stats and more contribution of the dehydrogenated nitrogen at the energy range [−1.95 −1.75]. We can thus expect that the nitrogen atom of the dehydrogenated NH group is also able to chemically bond with the substrate surface. Note that the DOS and PDOS analysis for the isolated thiolate anion (MBI^-) shows similar characteristics than MBIH species, and is not detailed here.

Adsorbed molecules at full coverage.—Figures 10 and 11 depict the ILDOS in different integral ranges, the PDOS on the molecule and for the S and N atoms for MBIH and MBI° adsorbed at full coverage, in the most stable adsorbed configurations (shown in Figs. 6a and 7a, respectively).

For MBIH (Fig. 10), the strong molecule-surface interactions is revealed by the drastic change in the DOS and PDOS of the molecules before and after adsorption. DOS after adsorption shows broadened and shifted peaks and the appearance of new peaks, due to the formation of chemical bonds between the molecules and the surface atoms. We can observe two energies range below the Fermi energy contains peaks dominated by the DOS of the sulfur atom. The ILDOS reveals that the peaks at range of [−2.00 −1.10] are similar to the sulfur contribution at HOMO and HOMO-1 before adsorption and that the peaks at range [−4.20 −3.40] are associated to the S–Cu_{cus} covalent bond. It can be concluded that the interaction via the sulfur atom is very strong and that it is the only atom in MBIH form involved in the formation of the covalent bond to the Cu(111)|| Cu_2O(111) surface.

For MBI° (Fig. 11), the drastic changes of the DOS and PDOS of the molecule before and after adsorption clearly show that the

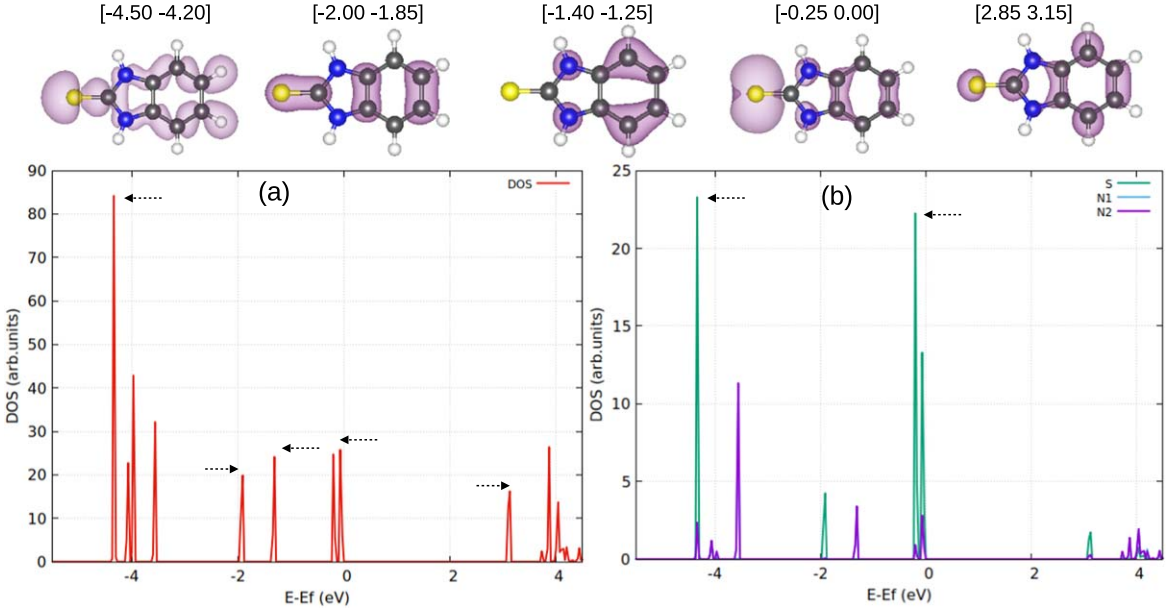

Figure 8. Electronic structure analysis of the isolated MBIH form: charge density associated with specific molecular orbitals (upper part), with the integration ranges, density of states (lower part (a)) and projected density of states for S and N atoms of the molecule (lower part (b)).

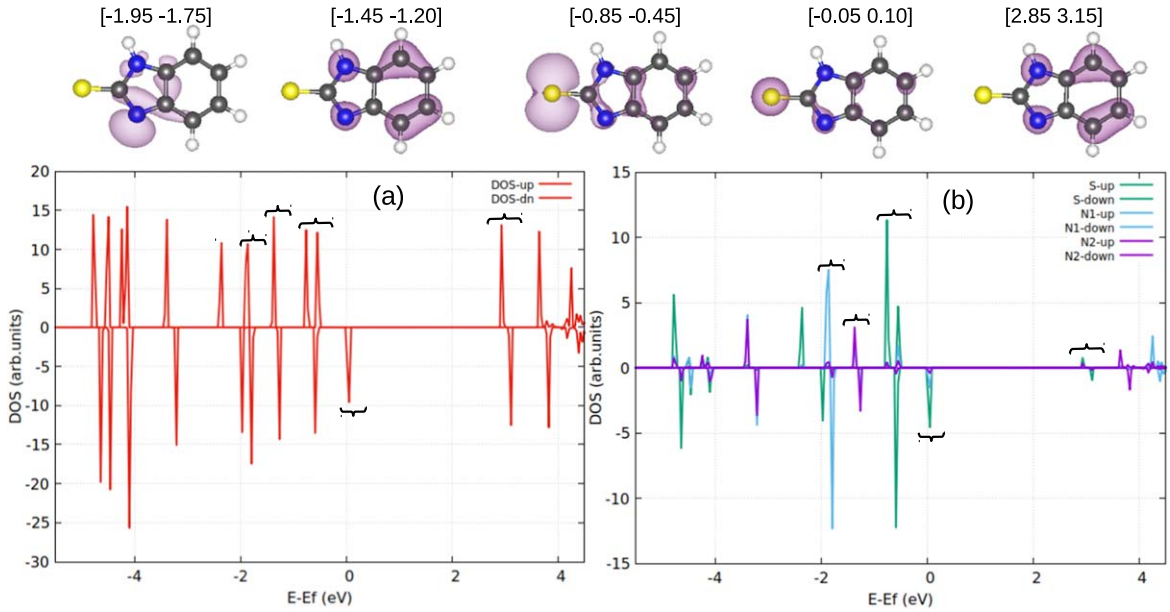

Figure 9. Electronic structure analysis of the isolated MBI° form: charge density associated with specific molecular orbitals (upper part), with the integration ranges, density of states (lower part (a)) and projected density of states for S and N atoms of the molecule (lower part (b)), N_1 corresponds to the deprotonated NH. Subscript up and down correspond to density of states for spin up and spin down, respectively.

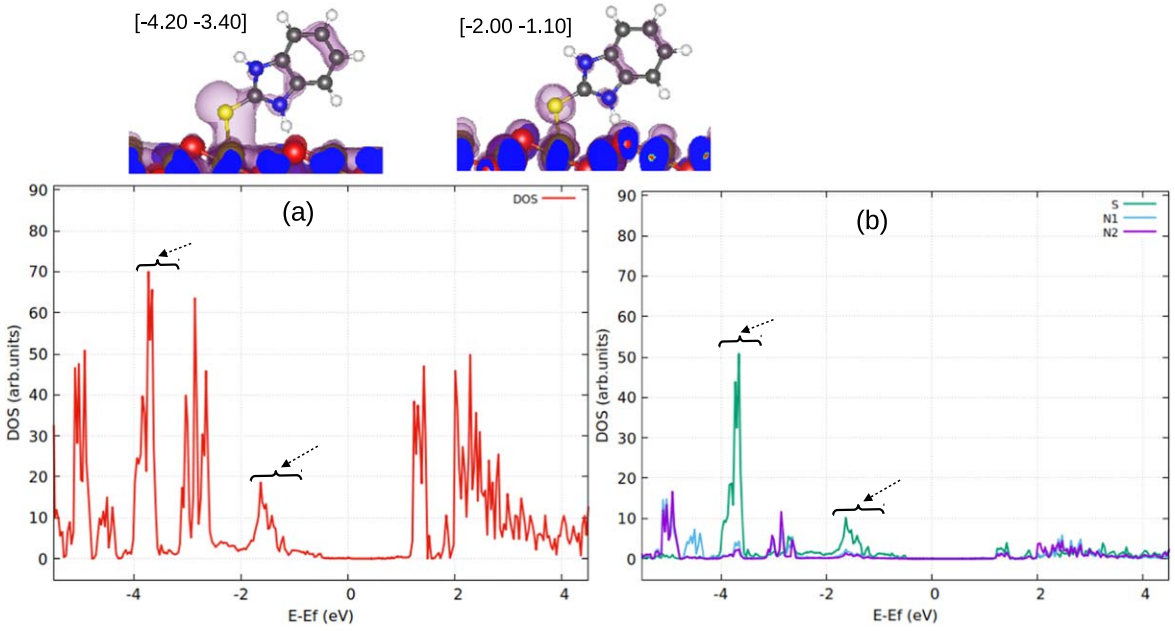

Figure 10. Electronic properties for the most stable adsorbed configuration of MBIH at full coverage: visualisation of integral local density of states (upper part), with integration ranges, projected density of states on the molecules (lower part (a)) and projected density of states for S and N atoms of the molecule (lower part (b)).

molecular states are also strongly affected by the adsorption process, which confirms the strong molecule-surface interaction. The broadened peaks located below the Fermi level in the energy range [−3.30 −2.35] correspond to the S–Cu_{cus} covalent bond and the broadened peaks located in the energy range [−5.20 −4.30] correspond principally to the N–Cu_{csa} chemical bond. Because the DOS at these peaks is dominated by sulfur and nitrogen states and the analysis is confirmed by ILDOS visualization, it can be concluded that both sulfur and nitrogen atoms are involved in the binding mechanism of MBI° adsorption on the preoxidized copper surface (Cu(111)|| Cu_2O(111)).

More details on the molecule-surface binding are provided by the charge density difference analysis. Figures 12a and 12b shows the charge density difference ($\Delta\rho(r)$), plotted with an isosurface of ±0.001 e $Å^{-3}$ for the most stable configurations of MBIH and MBI° at full coverage, respectively.

For MBIH, Fig. 12a shows charge density accumulation between the S and Cu_{cus} atoms and charge density depletion on the S and Cu_{cus} atoms, confirming again the formation of a S–Cu_{cus} covalent bond. NH...O_{up} H-bonding is confirmed by the observation of the charge density accumulation on one unsaturated oxygen atom and charge density depletion on the hydrogen of the NH group. For MBI°, Fig. 12b confirms the formation of two covalent bonds. We observe the charge density accumulation between the S and Cu_{cus} atoms for the S–Cu_{cus} bond and between the N and Cu_{csa} atoms for the N–Cu_{csa} bond.

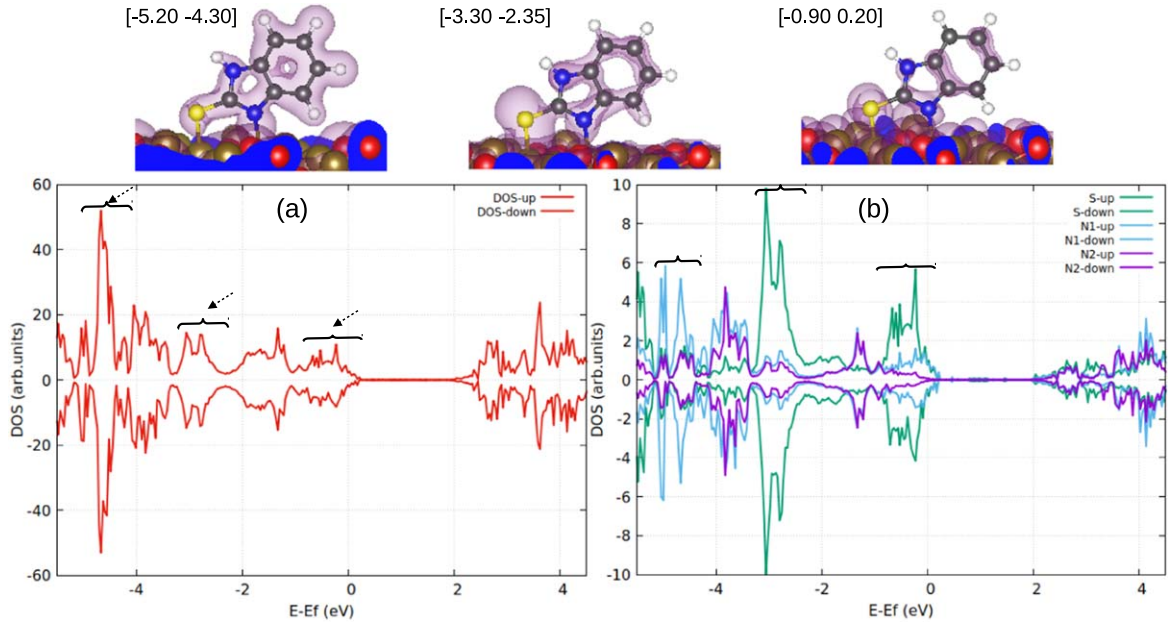

Figure 11. Electronic properties for the most stable configuration of MBI° form at full coverage: visualisation of integral local density of states (upper part), with the integration ranges, projected density of states on the molecules (lower part (a)) and projected density of states for S and N atoms of the molecule (lower part (b)). N_1 corresponds to the deprotonated NH. Subscript up and down correspond to density of states for spin up and spin down, respectively.

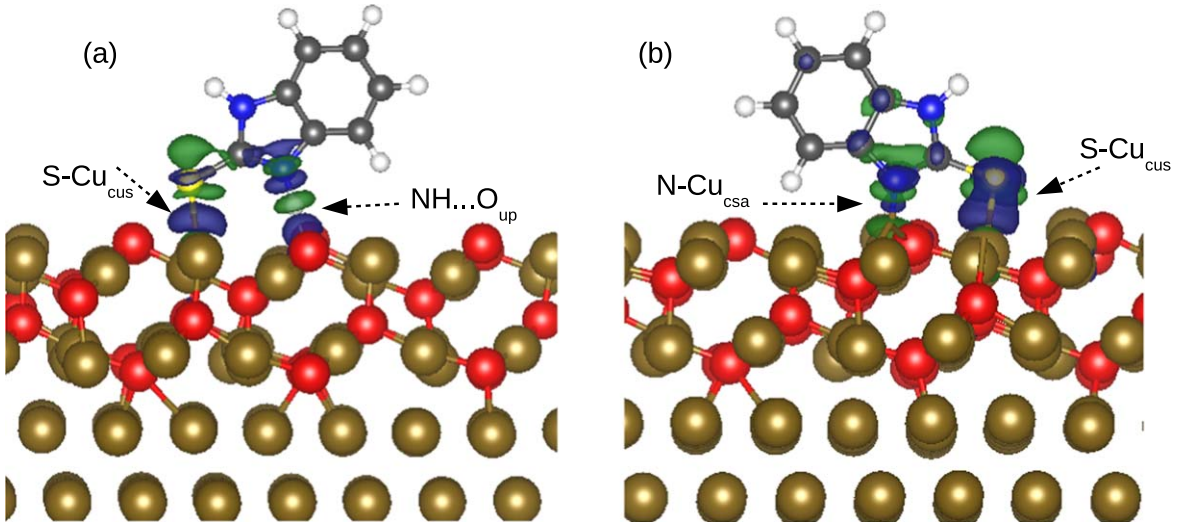

Figure 12. Charge density difference analysis for the most stable adsorbed configuration of MBIH (a) and MBI° (b) at full coverage. Blue and green color correspond to accumulation and deficit of charge density, respectively. For better visualization of the isosurface, only one molecule is represented in the same adsorption topology as at full coverage.

Table III summarizes the Bader charge analysis for the most stable adsorbed configurations of MBIH and MBI° at low and full coverages. The Bader charge analysis for MBIH form reveals an electron transfer from the organic layer to the oxide. In contrast for MBI°, we observed an electron transfer from the substrate to the organic layer, due to the radical form of the species considered in this case. For MBIH form, each molecule looses 0.28 and 0.16 e molecule^{-1} at low and full coverage, respectively. The electrons are redistributed principally in the oxide part of the substrate, whereas the electrons distribution in the metallic part shows no significant change after adsorption. For MBI° form, each molecule gains 0.29 and 0.34 e molecule^{-1} at low and full coverage, respectively, and the electrons come principally from the oxide part of the substrate.

Conclusions

DFT was used to investigate the adsorption of 2-mercaptobenzimidazole (MBI) organic inhibitor in thione (MBIH) and thiolate (MBI°) forms at low and full coverage on a preoxidized copper surface modeled by a Cu(111)|| Cu_2O(111) slab. At full coverage, we considered the oxide surface in the dry, hydrated and hydroxylated states. The structural and energetic trends were analyzed to determine the most stable adsorption configuration and more details about the molecule-surface interaction were provided by the electronic structure analysis.

The adsorption energy shows strong interaction of MBI with the Cu(111)|| Cu_2O(111) surface and the normalization of the adsorption energy to a unit area shows that full monolayer formation is favored

Table III. Bader charge analysis for the most stable adsorbed configurations of MBIH and MBI° at low and full coverage on preoxidized copper surface (Cu(111)|| Cu_2O(111)). ΔQ_{mol}, ΔQ_{oxide} and ΔQ_{metal} correspond to the Bader charge analysis on the molecule, oxide and metal parts, respectively, in e molecule^{-1}.

MBI species	coverage	ΔQ_{mol}	ΔQ_{oxide}	ΔQ_{metal}	Figures
MBIH	0.37 molecule nm^{-2}	+0.28	−0.22	−0.06	Fig. 4a
	3.27 molecule nm^{-2}	+0.16	−0.12	−0.04	Fig. 6b
MBI°	0.37 molecule nm^{-2}	−0.29	+0.25	+0.04	Fig. 5a
	3.27 molecule nm^{-2}	−0.34	+0.32	+0.02	Fig. 7b

compared to low coverage adsorption. At low coverage, the molecular plane of adsorbed MBI is tilted with respect to the surface plane, whereas at full coverage it is perpendicular for both MBIH and MBI° species. The sulfur atom is the most reactive site of MBI and it is covalently bonded to a Cu_{cus} surface atom, whatever the thione or thiolate forms of MBI and the surface coverage.

At low coverage, MBIH species also bind via H-bonding between one NH group and a O_{up} atom. For MBI° a carbon atom in the aromatic ring is also involved in the interaction mechanism and binds to an adjacent Cu_{cus} atom. MBI° also forms a chemical bond between the N atom and Cu_{csa}, instead of the NH...O_{up} H-bond for MBIH.

At full coverage, the molecules can form a dense and ordered monolayer with their plane perpendicular to the surface. MBIH forms one S–Cu_{cus} covalent bond and the orientation of the molecule on the Cu(111)|| Cu_2O(111) surface favors the formation of a NH–O_{up} H-bond. MBI° forms two covalent bonds via the S atom to Cu_{cus} and via the N atom to Cu_{csa}, which increases its bonding to the substrate compared to MBIH.

The strong adsorption and the formation of chemical bonds of MBI on the Cu(111)|| Cu_2O(111) surface were confirmed by the electronic analysis. The drastic changes in the DOS, ILDOS and charge density difference before and after adsorption highlights the formation of strong bonds between the molecule and the oxidized copper surface. Our calculations suggest that the substitution of water or OH groups by MBI is favored whatever the surface state of the oxide film.

Comparison with the data obtained on the same model oxidized copper surface with the MBT organic inhibitor shows similar bonding configurations at high coverage involving sulfur, N atoms and NH group, but MBI under thiolate form displays stronger adsorption bonding, owing to the substitution of endocyclic sulfur atom by an NH group. The dissociation mechanism for MBI at low coverage shows that the dissociation adsorption is more stable than the intact adsorption, which contrasts with the results on MBT that showed that the competitive adsorption is favored only in the presence of both species in the reacting phase. All these results suggest the strong adsorption of the MBI molecule under thione and thiolate form on copper covered by an ultra thin oxide film and contribute to explain the corrosion protection efficiency of the MBI molecule.

Acknowledgments

This project has received funding from the European Research Council (ERC) under the European Union's Horizon 2020 research and innovation program (ERC Advanced grant no. 741 123, Corrosion Initiation Mechanisms at the Nanometric and Atomic Scales : CIMNAS). GENCI is acknowledged for high performance calculations in thenational (IDRIS, CINES) centers under the project c2020082217.

ORCID

Dominique Costa https://orcid.org/0000-0002-3781-9867
Philippe Marcus https://orcid.org/0000-0002-9140-0047

References

1. D. Chadwick and T. Hashemi, "Electron spectroscopy of corrosion inhibitors: surface films formed by 2-mercaptobenzothiazole and 2-mercaptobenzimidazole on copper." *Surf. Sci.*, **89**, 649 (1979).
2. M. Finšgar, "2-mercaptobenzimidazole as a copper corrosion inhibitor: Part I. Long-term immersion, 3D-profilometry, and electrochemistry." *Corros. Sci.*, **72**, 82 (2013).
3. I. Milošev, N. Kovačević, J. Kovač, and A. Kokalj, "The roles of mercapto, benzene and methyl groups in the corrosion inhibition of imidazoles on copper: I. experimental characterization." *Corrosion Science*, **98**, 107 (2015).
4. G. Žerjav and I. Milošev, "Protection of copper against corrosion in simulated urban rain by the combined action of benzotriazole, 2-mercaptobenzimidazole and stearic acid." *Corrosion Science*, **98**, 180 (2015).
5. M. M. Musiani and G. Mengoli, "An electrochemical and SERS investigation of the influence of pH on the effectiveness of some corrosion inhibitors of copper." *J. Electroanal. Chem.*, **217**, 187 (1987).
6. P. M. Niamien, F. K. Essy, A. Trokourey, A. Yapi, H. K. Aka, and D. Diabate, "Correlation between the molecular structure and the inhibiting effect of some benzimidazole derivatives." *Mater. Chem. Phys.*, **136**, 59 (2012).
7. N. Kovačević, I. Milošev, and A. Kokalj, "The roles of mercapto, benzene, and methyl groups in the corrosion inhibition of imidazoles on copper: II. inhibitor-copper bonding." *Corrosion Science*, **98**, 457 (2015).
8. N. Kovačević and A. Kokalj, "Analysis of molecular electronic structure of imidazole- and benzimidazole-based inhibitors: a simple recipe for qualitative estimation of chemical hardness." *Corrosion Science*, **53**, 909 (2011).
9. S. Sun, Y. Geng, L. Tian, S. Chen, Y. Yan, and S. Hu, "Density functional theory study of imidazole, benzimidazole and 2-mercaptobenzimidazole adsorption onto clean Cu(111) surface." *Corrosion Science*, **63**, 140 (2012).
10. T. Shahrabi, H. Tavakholi, and M. G. Hosseini, "Corrosion inhibition of copper in sulphuric acid by some nitrogen heterocyclic compounds." *Anti-Corrosion Methods and Materials*, **54**, 308 (2007).
11. F. X. Perrin and J. Pagetti, "Characterization and mechanism of direct film formation on a Cu electrode through electro-oxidation of 2-mercaptobenzimidazole." *Corrosion Science*, **39**, 0536 (1998).
12. B. Trachli, M. Keddam, H. Takenouti, and A. Srhiri, "Protective effect of electropolymerized 2-mercaptobenzimidazole upon copper corrosion." *Progress in Organic Coatings*, **44**, 17 (2002).
13. J. Izquierdo, J. J. Santana, S. González, and R. M. Souto, "Scanning microelectrochemical characterization of the anti-corrosion performance of inhibitor films formed by 2-mercaptobenzimidazole on copper." *Progress in Organic Coatings*, **74**, 526 (2012).
14. D. q. Zhang, L. x. Gao, and G. d. Zhou, "Inhibition of copper corrosion in aerated hydrochloric acid solution by heterocyclic compounds containing a mercapto group." *Corrosion Science*, **46**, 3031 (2004).
15. J. D. G. Xue, X. Y. Huang, and J. Zhang, "The formation of an effective anti-corrosion film on copper surfaces from 2-mercaptobenzimidazole solution." *J. Electroanal. Chem. Interfacial Electrochem.*, **310**, 139 (1991).
16. M. Finšgar, "2-mercaptobenzimidazole as a copper corrosion inhibitor: Part II. surface analysis using X-ray photoelectron spectroscopy." *Corros. Sci.*, **72**, 90 (2013).
17. P. M. Niamien, H. A. Kouassi, A. Trokourey, F. K. Essy, D. Sissouma, and Y. Bokra, "Copper corrosion inhibition in 1 M HNO_3 by two benzimidazole derivatives." *ISRN, Materials Science*, **2012**, 623754 (2012).
18. I. B. Obot, Z. M. Gasem, and S. A. Umoren, "Understanding the mechanism of 2-mercaptobenzimidazole adsorption on Fe (110), Cu (111) and Al (111) surfaces: DFT and molecular dynamics simulations approaches." *Int. J. Electrochem. Sci.*, **9**, 2367 (2014), WOS:000334492800014.
19. E. Vernack, D. Costa, P. Tingaut, and P. Marcus, "DFT studies of 2-mercapto-benzothiazole and 2-mercaptobenzimidazole as corrosion inhibitors for copper." *Corros. Sci.*, **174**, 108840 (2020).
20. F. Chiter, D. Costa, V. Maurice, and P. Marcus, "DFT investigation of 2-mercaptobenzothiazole adsorption on model oxidized copper surfaces and relationship with corrosion inhibition." *Appl. Surf. Sci.*, **537**, 147802 (2020).
21. G. Sun, J. Kürti, P. Rajczy, M. Kertesz, J. Hafner, and G. Kresse, "Performance of the vienna ab initio simulation package (VASP) in chemical applications." *J. Mol. Struct. THEOCHEM*, **624**, 37 (2003).
22. G. Kresse and J. Hafner, *Phys. Rev. B*, **47**, 558 (1993).
23. G. Kresse and J. Furthmüller, "Efficiency of ab-initio total energy calculations for metals and semiconductors using a plane-wave basis set." *Comput. Mater. Sci.*, **6**, 15 (1996a).
24. G. Kresse and J. Furthmüller, "Efficient iterative schemes for ab initio total-energy calculations using a plane-wave basis set." *Phys. Rev. B*, **54**, 11169 (1996b).
25. J. Klimeš, D. R. Bowler, and A. Michaelides, "Van der Waals density functionals applied to solids." *Phys. Rev. B*, **83**, 195131 (2011).
26. C. Kittel, *Introduction to Solid State Physics* (Wiley Sons, New York) 7th ed. (1996), https://books.google.fr/books/about/Introduction_to_Solid_State_Physics.html?id=1X8pAQAAMAAJ&redir_esc=y9780471111818.
27. A. Werner and H. D. Hochheimer, "High-pressure X-ray study of Cu20 and Ag20." *Phys. Rev. B*, **25**, 5929 (1982).

28. F. Chiter, D. Costa, V. Maurice, and P. Marcus, "A DFT-based Cu(111)|| Cu_2O(111) model for copper metal covered by ultrathin copper oxide: structure, electronic properties and reactivity." *J. Phys. Chem. C*, **124**, 17048 (2020).
29. K. Ravikumar, K. C. Mohan, M. Bidyasagar, and G. Y. S. K. Swamy, "Crystal structure of 2-mercaptobenzimidazole and bis[2- mercaptobenzimidazole]dichlorocobalt(II)." *Journal of Chemical Crystallography*, **26**, 325 (1995).
30. A. L. R. Silva and M. D. M. C. R. da Silva, "Energetic, structural and tautomeric analysis of 2-mercaptobenzimidazole." *J Therm Anal Calorim*, **129**, 1679 (2017).
31. G. Liu, H. Zeng, Q. Lu, H. Zhong, P. Choi, and Z. Xu, "Adsorption of mercaptobenzoheterocyclic compounds on sulfide mineral surfaces: a density functional theory study of structure-reactivity relations." *Colloids and Surfaces A: Physicochem. Eng. Aspects*, **409**, 1 (2012).
32. G. A. Zhang, X. M. Hou, B. S. Hou, and H. F. Liu, "Benzimidazole derivatives as novel inhibitors for the corrosion of mild steel in acidic solution: experimental and theoretical studies." *Journal of Molecular Liquids*, **278**, 413 (2019).
33. W. Tang, E. Sanville, and G. Henkelman, "A grid-based bader analysis algorithm without lattice bias." *J. Phys.: Condens. Matter*, **21**, 084204 (2009).